

Bragg diffraction of microcavity polaritons by a surface acoustic wave

Kikuo Cho and Kazunori Okumoto

Graduate School of Engineering Science, Osaka University, 1-3 Machikaneyama, Toyonaka 560-8531, Japan

N. I. Nikolaev and A. L. Ivanov

Department of Physics and Astronomy, Cardiff University, Cardiff CF24 3YB, United Kingdom

(Dated: July 9, 2018)

Bragg scattering of polaritons by a coherent acoustic wave is mediated and strongly enhanced by the relevant exciton states resonant with the acoustic and optic fields simultaneously. In this case, in sharp contrast with conventional acousto-optics, the resonantly enhanced Bragg spectra reveal the multiple orders of diffracted light, i.e., a Brillouin band structure of parametrically driven polaritons can be directly visualized. We analyze the above scheme for polaritons in (GaAs) semiconductor microcavities driven by a surface acoustic wave (SAW) and show that for realistic values of the SAW, $\nu_{\text{SAW}} = 1$ GHz and $I_{\text{ac}} \lesssim 100$ W/cm², the main acoustically-induced band gap in the polariton spectrum can be as large as $\Delta_{\text{ac}}^{\text{MC}} \simeq 0.6$ meV, and the Bragg replicas up to $n = 3$ can be observed.

PACS numbers: 71.36.+c, 42.65.Es, 43.60.+d

Back in 1933, Léon Brillouin, a founder of acousto-optics, described for the first time non-perturbative solutions of the Maxwell wave equation for the dielectric constant ε harmonically modulated by an acoustic wave $\{\mathbf{k}, \Omega_{\mathbf{k}}^{\text{ac}}\}$, i.e., for $\varepsilon = \varepsilon_b + \delta\varepsilon_b \cos(\Omega_{\mathbf{k}}^{\text{ac}}t - \mathbf{k}\mathbf{r})$ [1]. Formally, the eigenvalues and eigenstates of the above equation are given in terms of the Mathieu functions and yield an infinite sequence of the alternating allowed and forbidden energy bands in momentum space. While the energy structure is akin to the electron energy bands, which appear in the presence of a periodic (atomic) potential, a very particular feature of the *harmonic* potential is that the forbidden energy bands, i.e., the acoustically-induced energy gaps $\Delta_{\text{ac}}^{(n)}$ ($n = 1, 2, \dots$) in the photon spectrum, extremely effectively close up with the increasing energy number n : $\Delta_{\text{ac}}^{(n)} \propto (\delta\varepsilon_b)^n$. This is an inherent property of the Mathieu wavefunctions [2]. The acousto-optic science deals with $\delta\varepsilon_b = 4\pi\chi_{\gamma\text{-ac}}^{(2)} I_{\text{ac}}^{1/2}$, where I_{ac} is the intensity of the acoustic wave and $\chi_{\gamma\text{-ac}}^{(2)}$ is a second-order non-resonant acousto-optic susceptibility [3, 4]. The non-resonant acousto-optic nonlinearities are small, so that usually $\delta\varepsilon_b \sim 10^{-4} - 10^{-3}$ (for GaAs, e.g., $\delta\varepsilon_b \simeq 1.6 \times 10^{-3}$ for $I_{\text{ac}} = 100$ W/cm²). As a result, the conventional acousto-optics, both fundamental and applied, attributes the Bragg diffraction of the light field by a sound wave to the one-phonon transition only, i.e., to the main acoustically-induced gap $n = 1$ [3, 4, 5, 6].

The nonresonant acousto-optic nonlinearities, which give rise to the acoustically-induced diffraction grating, is due to the photoelastic effect. In sharp contrast with this mechanism, the *resonant acousto-optic effect* [7, 8] for bulk and microcavity (MC) polaritons deals with a quantum diffraction of optically-induced, virtual excitons by the coherent acoustic wave. In this case the interaction of two “matter” waves, the excitonic polarization and the acoustic field, is much more effective than

the nonresonant photoelastic coupling of photons with acoustic phonons. In the meantime the photon component of optically-dressed excitons, i.e., of polaritons, can be large enough to ensure an efficient resonant conversion “photon \leftrightarrow exciton”. This explains the origin of the resonant, exciton-mediated acousto-optic nonlinearity, $\delta\varepsilon_{\gamma\text{-ac}}^x \gg \delta\varepsilon_b$. For GaAs-based structures at low temperatures $\delta\varepsilon_{\gamma\text{-ac}}^x$ can be as large as $\delta\varepsilon_{\gamma\text{-ac}}^x \sim 0.1$. Thus the resonant acousto-optics of polaritons deals with the microscopic mechanism fundamentally different from the photoelastic effect.

In this Letter we propose and calculate the acousto-optic Bragg scattering of SAW-driven polaritons. The MC polariton eigenstates in GaAs λ -cavities [9, 10, 11] are relevant to the proposed Bragg spectroscopy, due to compatibility of GaAs microcavities with the SAW technique [12] and due to a possibility to realize one-dimensional geometry for the resonant, SAW-mediated interaction of two counter-propagating MC polaritons by using $\nu_{\text{SAW}} \lesssim 3$ GHz [8]. As we demonstrate below, the Bragg spectra of MC polaritons are resonantly enhanced by the quantum well (QW) exciton state and consist of the well-developed multiple replicas with a robust structure.

For the acousto-optic spectroscopy of polaritons, both resonant interactions, the exciton-photon coupling and the interaction of excitons with the acoustic pump wave, should be treated non-perturbatively (strong coupling regime) and on an equal basis. Being applied to the Bragg scattering of MC polaritons, the acousto-optic polariton macroscopic equations [7] are given by

$$\left[\frac{\partial^2}{\partial x^2} + \frac{\partial^2}{\partial z^2} - \frac{\varepsilon_b(z)}{c^2} \frac{\partial^2}{\partial t^2} \right] E = \frac{4\pi}{c^2} \frac{\partial^2}{\partial t^2} P + J_{\text{ext}}, \quad (1)$$

$$\left[\frac{\partial^2}{\partial t^2} + 2\gamma_x \frac{\partial}{\partial t} + \omega_{\text{T}}^2 - \frac{\hbar\omega_{\text{T}}}{M_x} \frac{\partial^2}{\partial x^2} - \right.$$

$$-4m_k^x \omega_T \cos(\Omega_k^{\text{ac}} t - kx) \Big] P = \Omega_{x-\gamma}^2 E, \quad (2)$$

where E and P are the light field and excitonic polarization, respectively, J_{ext} is a source of the external optical wave necessary for the Bragg scattering problem, $\hbar\omega_T$ is the energy position of the exciton line, M_x is the in-plane translational mass of QW excitons, $\Omega_{x-\gamma}$ is the matrix element of the QW exciton – MC photon interaction, and $2\gamma_x = 1/T_1 = 2/T_2$ is the rate of incoherent scattering of QW excitons. We assume a Cartesian coordinate system with the in-plane x -axis along the SAW wavevector \mathbf{k} , the z -axis along the MC growth direction, and the exciton and light fields linearly polarized along the in-plane y -axis. In this case the SAW, which has both transverse and longitudinal displacement components, u_x and u_z , is elliptically-polarized in the x - z plane (the sagittal plane).

The SAW-induced modulation of the excitonic polarization is characterized by the coupling coefficient $m_k^x = I_{\text{ac}}^{1/2} [|u_x| / (|u_x|^2 + |u_z|^2)^{1/2}] |m_{x-\text{ac}}^{\text{DP}} + i\gamma_{\text{SAW}} m_{x-\text{ac}}^{\text{PE}}|$, where $m_{x-\text{ac}}^{\text{DP}}$ and $m_{x-\text{ac}}^{\text{PE}}$ are the deformation potential (DP) and piezoelectric (PE) matrix elements of exciton – SAW interaction, respectively, and $\gamma_{\text{SAW}} = |u_z|/|u_x| \exp(i\delta_{\text{SAW}})$. The phase shift δ_{SAW} between u_x and u_z is nearly $\pi/2$ [12], so that both interaction channels interfere constructively. However, because $m_{x-\text{ac}}^{\text{DP}} \gg m_{x-\text{ac}}^{\text{PE}}$ (for $\nu_{\text{SAW}} \lesssim 10$ GHz) and $|u_z|/|u_x| \simeq 1.4$ [13], the DP mechanism with $m_{x-\text{ac}}^{\text{DP}} = D_x / (2\hbar^2 \rho v_s^3)^{1/2}$ is strongly dominant over the PE one. Here, ρ is the crystal density, v_s is the SAW velocity, and D_x is the exciton – LA-phonon DP. The above hierarchy of the interaction mechanisms is due to the charge neutrality of excitons: In contrast, the electron – SAW interaction is determined by the PE coupling [13].

The z -dependent background dielectric function $\varepsilon_b(z)$ on the left-hand-side (l.h.s.) of Eq.(1) refers to a stack of layers which form the MC structure we analyze, i.e., a GaAs λ -cavity with an embedded InGaAs QW, symmetrically sandwiched in between two identical AlGaAs/AlAs Bragg reflectors. The Bragg reflectors give rise to the transverse optical confinement and, in the meantime, ensure an optical coupling of the external light wave with the in-plane polariton quasi-eigenstates. At first, however, in order to visualize the quasi-energy spectrum of SAW-driven MC polaritons, we assume 100% optical confinement (i.e., replace the Bragg reflectors by perfect mirrors), no external light source [i.e., $J_{\text{ext}} = 0$ on the r.h.s. of Eq.(1)], and no damping of the exciton states [i.e., $\gamma_x = 0$ on the l.h.s. of Eq.(2)]. In this case the polariton spectrum is characterized by the MC Rabi frequency $\Omega_x^{\text{MC}} = 2(\pi/\varepsilon_b)^{1/2} \Omega_{x-\gamma}$. In Fig.1 we plot the quasi-energy spectrum of lower-branch (LB) polaritons in a zero detuning MC with $\Omega_x^{\text{MC}} = 3.7$ meV, driven by the SAW of $\nu_{\text{SAW}} = 1$ GHz and $I_{\text{ac}} = 10$ W/cm².

The quasi-energy spectrum, which is calculated by the

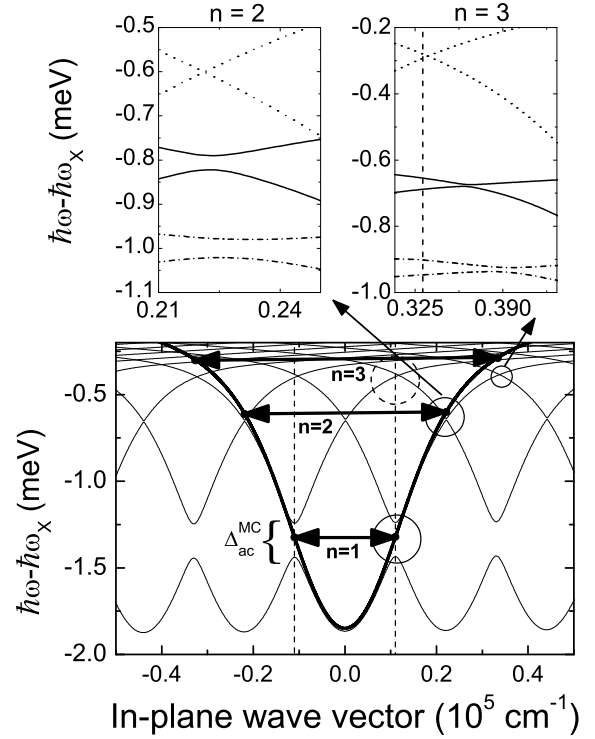


FIG. 1: The acoustically induced quasi-energy spectrum of polaritons in a GaAs λ -microcavity driven by the SAW of $\nu_{\text{SAW}} = 1$ GHz, $k = 2.2 \times 10^4$ cm⁻¹, $I_{\text{ac}} = 10$ W/cm², $v_s = 2.9 \times 10^5$ cm/s, and $D_x = 12$ eV (thin solid lines). The initial, acoustically-unperturbed lower dispersion branch of MC polaritons is shown by the bold solid line. The MC Rabi energy is $\hbar\Omega_x^{\text{MC}} = 3.7$ meV. The magnified energy bands relevant to the resonant $n = 2$ and 3 transitions are plotted in the l.h.s. and r.h.s. upper insets, respectively, for $I_{\text{ac}} = 0$ (dotted lines), $I_{\text{ac}} = 50$ W/cm² (solid lines), and $I_{\text{ac}} = 100$ W/cm² (dash-dotted lines). The vertical dashed lines show the boundaries of the acoustically-induced first Brillouin zone.

method developed in Ref. [7] for bulk polaritons and cannot be interpreted in terms of the Mathieu functions, show the acoustically-induced band gaps $\Delta_{\text{ac}}^{\text{MC}(n)} \propto I_{\text{ac}}^{n/2}$, due to the $n = 1, 2, \dots$ – phonon-assisted transitions. Because the energy of SAW phonons is very small, $\hbar\nu_{\text{SAW}} \simeq 4.1$ μ eV only, the acoustically-induced spectral gaps refer to the in-plane counter-propagating MC polariton states $\{nk/2, \omega_{\text{LB}}^{\text{MC}}(nk/2)\}$ and $\{-nk/2, \omega_{\text{LB}}^{\text{MC}}(nk/2)\}$ (see the nearly horizontal arrows in Fig.1), where $\omega_{\text{LB}}^{\text{MC}}(p_{\parallel})$ with $p_{\parallel} = \pm nk/2$ is the LB solution of the dispersion equation $c^2 p_{\parallel}^2 / \varepsilon_b + \omega_T^2 - \omega^2 = (\omega_{\text{ac}}^{\text{MC}})^2 / (\omega_T^2 + \hbar\omega_T p_{\parallel}^2 / M_x - \omega^2)$. The main acoustically-induced band gap in the LB spectrum is given by $\Delta_{\text{ac}}^{\text{MC}} \equiv \Delta_{\text{ac}}^{\text{MC}(n=1)} = 2|m_k^x| \varphi^{\text{MC}}(k/2)$, where $\varphi^{\text{MC}}(k/2) = (\Omega_x^{\text{MC}})^2 / \{(\Omega_x^{\text{MC}})^2 + 4[\omega_T - \omega_{\text{LB}}^{\text{MC}}(k/2)]^2\}$ is the excitonic component of the polariton states $p_{\parallel} = \pm k/2$ resonantly coupled via one-SAW-phonon transition. Even for modest SAW intensities the main gap is large, so that $\Delta_{\text{ac}}^{\text{MC}} \gg \hbar\nu_{\text{SAW}}$. For

example, $I_{ac} = 100 \text{ W/cm}^2$ yields $\Delta_{ac}^{MC}/\hbar \simeq 130 \text{ GHz}$. Note, that the conventional acousto-optics deals with the acoustically-induced stop gap $\Delta_{\gamma-ac}$ less than the SAW frequency (usually, $\Delta_{\gamma-ac} \lesssim 100 \text{ MHz}$) [4, 12]. Furthermore, the acoustic band gaps associated with the two- and three-phonon transitions in the MC polariton spectrum are also well developed, so that $\Delta_{ac}^{MC(n=1)} : \Delta_{ac}^{MC(n=2)} : \Delta_{ac}^{MC(n=3)} = 1 : 0.08 : 0.03$ for $I_{ac} = 100 \text{ W/cm}^2$ (see the insets of Fig. 1). This is in a sharp contrast with the traditional acousto-optic schemes of the Bragg scattering. All the above features of the quasi-energy spectrum of SAW-driven MC polaritons are due to the resonant, exciton-mediated acousto-optic susceptibility.

Due to the periodicity of the acoustic wave, the quasi-energy spectrum can also be interpreted in terms of an *extended* Brillouin zone, with the band boundaries at $p_{\parallel} \simeq \pm nk/2$. The first acoustically-induced Brillouin zone is shown in Fig. 1 by the vertical dashed lines. The energy band boundaries, where the spectral gaps arise and develop with increasing I_{ac} , can be probed in Bragg scattering, by changing the incidence angle α of the external optical wave. At this point we return to Eqs. (1)-(2) applied to a realistic MC structure with the Bragg reflectors consisting of 34 alternating AIsAs and $\text{Al}_{0.13}\text{Ga}_{0.87}\text{As}$ $\lambda/4$ -layers. The MC polariton quasi-eigenstates can now be excited by the external light field, $E_{inc} = E_{inc}^{(0)} e^{-i\omega t}$ [due to the J_{ext} -term on the r.h.s. of Eq. (1)], and can decay or scatter into the external electromagnetic modes.

In order to calculate the SAW-induced Bragg diffraction of optically excited MC polaritons, we use the Green function technique developed in Ref. [14]. Because the in-plane wavevector p_{\parallel} is conserved in the propagation of the light field through an optically transparent planar structure, one defines the MC photon Green function $g(z, z'; \omega)$ by the equation:

$$\frac{d^2}{dz^2} g(z, z'; \omega) + \kappa^2 g(z, z'; \omega) = -4\pi\delta(z - z'), \quad (3)$$

where $\kappa^2 = (\omega/c)^2 \varepsilon_b(z) - p_{\parallel}^2$. The function $g(z, z'; \omega)$, which satisfies the Maxwellian boundary conditions, is evaluated numerically with the use of $\varepsilon_b(z)$ relevant to the MC structure we analyze. As a next step, we substitute in Eqs. (1)-(2) a Fourier expansion of the E and P fields in terms of the in-plane quasi-wavevector $p_{\parallel} + \ell k$ and quasi-frequency $\omega + 2\pi\ell\nu_{\text{SAW}}$, and evaluate the SAW-mediated acousto-optic susceptibility matrix $\chi_{\ell, \ell'}$: $P_{\ell} = \sum_{\ell'} \chi_{\ell, \ell'} E_{\ell'}$ ($\ell = 0, \pm 1, \dots$, i.e., $\ell = \pm n$ corresponds to the n -phonon transition). The acoustically-induced polarization harmonics P_{ℓ} give rise to the Bragg signal:

$$E_{\ell} = E_{\ell}^{(0)} + q_{\ell}^2 \int dz' g(z, z', \omega_{\ell}) \sum_{\ell'} \chi_{\ell, \ell'} E_{\ell'}(z'), \quad (4)$$

where $q_{\ell}^2 = (\omega + 2\pi\ell\nu_{\text{SAW}})^2/c^2$, $E_{\ell} = E_{\ell}(z)$ is the signal light field, and $E_{\ell}^{(0)} = E_{\ell}^{(0)}(z)$ is the incoming light

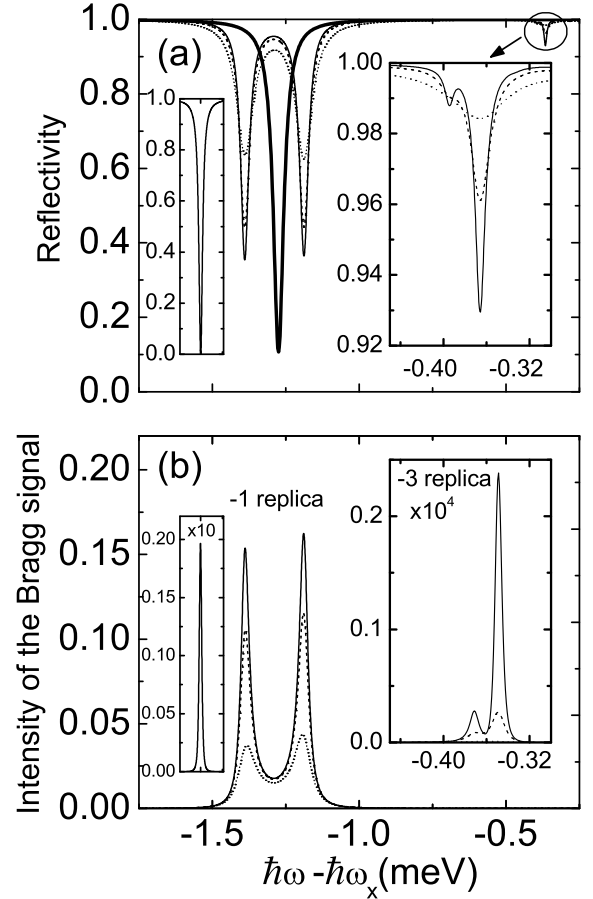


FIG. 2: The Bragg spectra of SAW-driven MC polaritons. The incident optical wave excites the MC polariton states at the r.h.s. boundary of the acoustically-induced first Brillouin zone (see Fig. 1), i.e., $p_{\parallel} = k/2$ and $\alpha = \alpha_B \simeq 8.2^\circ$. (a) The reflection coefficient $|r(\omega, I_{ac})|^2$ of the optical wave against the frequency ω . The thick solid line shows the initial polariton-mediated MC reflectivity for $I_{ac} = 0$ and $\gamma_x = 10 \mu\text{eV}$. The thin lines refer to $|r(I_{ac}=10 \text{ W/cm}^2)|^2$ for spectral vicinity of $n = 1$ SAW-phonon transition. Inset: $|r|^2$ for spectral vicinity of $n = 3$ SAW-phonon transition. (b) The -1 and -3 Bragg diffraction replicas normalized to I_{opt} . The l.h.s. inset: -1 Bragg replica calculated by using the nonresonant $\chi_{\gamma-ac}^{(2)}$. The solid, dashed and dotted lines refer to the excitonic damping $\hbar\gamma_x = \hbar/T_2 = 5, 10, \text{ and } 30 \mu\text{eV}$, respectively.

field induced by E_{inc} . The field $E_{\ell}^{(0)}(z)$ is calculated by using the photon Green function defined by Eq. (3). The integration on the r.h.s. of Eq. (4) is over the QW thickness, so that one can approximate $E_{\ell'}(z')$ by $E_{\ell'}(z'=0)$. The latter amplitude is evaluated from Eq. (4) by putting $z = 0$. Finally, the outgoing, diffracted field E_{ℓ} is calculated from the completely defined r.h.s. of Eq. (4).

The Bragg angle Θ_B corresponds to the effective SAW-induced diffraction of MC polaritons with $p_{\parallel} = \pm k/2$ and is given by $\sin \Theta_B = [k/(2k_{opt})] \{1 - [(v_s k)/(8\varepsilon_b \omega_T)] [(ck)/\Omega_x^{MC}]^2\} \simeq k/(2k_{opt})$, where $k_{opt} =$

ω/c is the wavevector of the external optical wave. In Fig. 2a we plot the reflection coefficient $|r(\omega, I_{ac})|^2$ of the incoming light incident at angle $\alpha = \Theta_B$ on the SAW-driven MC ($\nu_{SAW} = 1$ GHz). In this case the r.h.s. boundary at $p_{\parallel} = k/2$ of the acoustically-induced first Brillouin zone is probed (see Fig. 1). In the vicinity of $\omega = \omega_{LB}^{MC}(k/2)$, with increasing I_{ac} the reflectivity changes its single-line shape for $I_{ac} = 0$ (the initial reflection spectrum is shown in Fig. 2a by the bold solid line) to a high contrast double-line shape with the separation Δ_{ac}^{MC} between two dips. Furthermore, a similar double-line structure, which refers to the three-phonon-assisted transition, appears and develops with increasing I_{ac} for the reflectivity at $\omega \simeq \omega_{LB}^{MC}(3k/2)$ (see the inset of Fig. 2a). Because the wavevector band $-k/2 \leq p_{\parallel} \leq k/2$ can also be interpreted in terms of the SAW-induced *reduced* Brillouin zone, the incident optical wave probes the odd-order SAW-induced energy gaps (the areas marked in Fig. 1 by large solid and dashed circles refer to the $n = 1$ and 3 transitions). The corresponding frequency-down-shifted -1 and -3 Bragg replicas give rise to the outgoing optical signal and are plotted in Fig. 2b. The camel-back shape of the replicas follow the band gaps Δ_{ac}^{MC} and $\Delta_{ac}^{MC(n=3)}$, respectively. In Fig. 3a, $|r(\omega, I_{ac})|^2$ is shown for $\alpha \simeq 2\Theta_B$, so that the r.h.s. boundary at $p_{\parallel} = k$ of the second (extended) Brillouin zone is probed. The corresponding -2 Bragg replica is plotted in Fig. 3b. In Figs. 3c-d we show the energy separation between two spikes in the -1 and -2 replicas. The separation is equal to $\Delta_{ac}^{MC} \propto I_{ac}^{1/2}$ and $\Delta_{ac}^{MC(n=2)} \propto I_{ac}$, respectively.

Bragg diffraction, due to the nonresonant $\chi_{\gamma-ac}^{(2)}$, has been observed for an optical wave guided by SAW-driven semiconductor layers [15, 16, 17]. The one-phonon diffraction replica -1 , calculated for the GaAs-based MC with the use of $\chi_{\gamma-ac}^{(2)}$, is plotted in the l.h.s. inset of Fig. 2b. In this case the acoustically-induced main stop gap in the MC photon spectrum is very small and completely screened by the radiative damping, so that it cannot be seen in the Bragg signal as a camel-back structure. Note that the SAW intensities I_{ac} we discuss are much less than those used to acoustically ionize, by the piezoelectric effect, the excitons in GaAs structures [18, 19].

For the analyzed scattering of MC polaritons by the SAW, the Klein-Cook parameter [4] $Q = Q(\omega)$, which distinguishes the Raman-Nath (transmission-type) regime from the Bragg (reflection-type) mode, is given by $Q = v_{pol}(\hbar/\gamma_{pol})(k^2/k_{opt})$. Here, $v_{pol}(\omega)$ and $\gamma_{pol}(\omega)$ are the MC polariton velocity and damping, respectively. For the case analyzed in Figs. 1-3, $Q \simeq 6.5 \gg 1$, i.e., our theory does deal with the Bragg diffraction regime.

We appreciate valuable discussions with Yu. Kosevich, Peter Littlewood, and W. Sohler. Support of this work by the CREST, Grant-in-Aid of the Ministry of Education of Japan, Toyota Phys. & Chem. Institute, and EU RTN Project HPRN-2002-00298 is gratefully acknowledged.

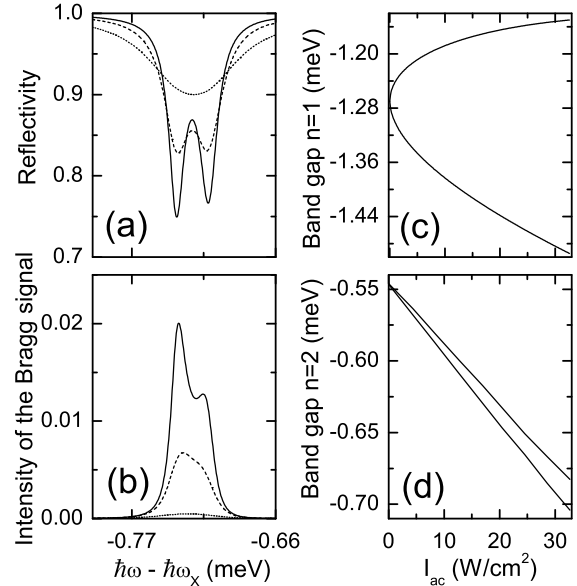


FIG. 3: The Bragg spectra of SAW-driven MC polaritons for $n = 2$ transition. (a) The reflection coefficient $|r(\omega, I_{ac})|^2$ for $\alpha = 16.8^\circ$ ($p_{\parallel} \simeq k$ and $\omega \simeq \omega_{LB}^{MC}(k)$, see Fig. 1), $\nu_{SAW} = 1$ GHz and $I_{ac} = 40$ W/cm². (b) The frequency-down-converted -2 Bragg replica. The solid, dashed and dotted lines refer to the excitonic damping $\hbar\gamma_x = \hbar/T_2 = 5, 10$, and $30 \mu\text{eV}$, respectively. (c)-(d) The SAW-induced spike separation, i.e., the band gaps $\Delta_{ac}^{MC(n=1)}$ and $\Delta_{ac}^{MC(n=2)}$, against I_{ac} .

-
- [1] L. Brillouin, *Actual. Sci. Ind.* **59** (1933).
 - [2] G. Blanch, in *Handbook of Mathematical Functions*, edited by M. Abramowitz and I. A. Stegun (Dover Publications, New York, 1965), p. 721.
 - [3] J. Wilson and J. F. B. Hawkes, *Optoelectronics* (Prentice Hall International, New Jersey, 1983), Sec. 3.8.
 - [4] A. Korpel, *Acousto-Optics*, Second Edition (M. Dekker, Inc., New York, 1997), Chap. 2 and 3.
 - [5] L. Brillouin, *Ann. Phys. (Paris)* **17**, 88 (1922).
 - [6] R. S. Chu and T. Tamir, *J. Opt. Soc. Am.* **66**, 220 (1976); R. S. Chu and J. A. Kong, *J. Opt. Soc. Am.* **70**, 1 (1980).
 - [7] A. L. Ivanov and P. B. Littlewood, *Phys. Rev. Lett.* **87**, 136403 (2001). Due to a misprint, the factor 2 in the last term on the l.h.s. of Eq. (4b) should be replaced by 4.
 - [8] A. L. Ivanov and P. B. Littlewood, *Semicond. Sci. Technol.* **18**, S428 (2003). In this paper only the PE exciton-phonon interaction is included for the SAW-induced scattering.
 - [9] M. S. Skolnick, T. A. Fisher, and D. M. Whittaker, *Semicond. Sci. Technol.* **13**, 645 (1998).
 - [10] J. J. Baumberg, *Phys. World* **15**, 37 (2002).
 - [11] A. Kavokin and G. Malpuech, *Cavity Polaritons* (Elsevier, Amsterdam, 2003).
 - [12] C. Campbell, *Surface Acoustic Wave Devices and Their Signal Processing Applications* (Academic, New York, 1989), Chap. 2.

- [13] S. H. Simon, Phys. Rev. B **54**, 13878 (1996).
- [14] K. Cho, *Optical Response of Nanostructures: Microscopic Nonlocal Theory* (Springer Verlag, Heidelberg, 2003), Sec. 3.4; J. Luminescence **102/103**, 232 (2003).
- [15] L. Kuhn, M. L. Dakss, P. F. Heidrich, and B. A. Scott, Appl. Phys. Lett. **17**, 265 (1970).
- [16] K. W. Loh, W. S. C. Chang, W. R. Smith, and T. Grudkowski, Appl. Opt. **15**, 156 (1976).
- [17] D. Ciplys, R. Rimeika, M. S. Shur, P. Gaska, J. Deng, J. Yang, and M. A. Khan, Appl. Phys. Lett. **80**, 1701 (2002).
- [18] C. Rocke, A. O. Govorov, A. Wixforth, G. Böhm, and G. Weimann, Phys. Rev. B **57**, R6850 (1998); C. Rocke, S. Zimmermann, A. Wixforth, J. P. Kotthaus, G. Böhm, and G. Weimann, Phys. Rev. Lett. **78**, 4099 (1997).
- [19] P. V. Santos, M. Ramsteiner, and F. Jungnickel, Appl. Phys. Lett. **72**, 2099 (1998).